THE ASTROPHYSICAL JOURNAL, 567:762–771, 2002 March 10

NONTHERMAL X-RAY EMISSION: AN ALTERNATIVE TO CLUSTER COOLING FLOWS?

IAN G. MCCARTHY,[1,2] MICHAEL J. WEST,[3] AND GARY A. WELCH[1]

Received 2001 April 16; accepted 2001 November 14

ABSTRACT

We report the results of experiments aimed at reducing the major problem with cooling flow models of rich cluster X-ray sources, i.e., the fact that most of the cooled gas or its products have not been found. Here we show that much of the X-ray emission usually attributed to cooling flows can, in fact, be modeled by a power-law component which is indicative of a source(s) other than thermal bremsstrahlung from the intracluster medium. We find that adequate simultaneous fits to *ROSAT* PSPC and *ASCA* GIS/SIS spectra of the central regions of 10 clusters are obtained for two-component models that include a thermal plasma component that is attributable to hot intracluster gas and a power-law component that is likely generated by compact sources and/or extended nonthermal emission. For five of the clusters that purportedly have massive cooling flows, the best-fit models have power-law components that contribute $\sim$30% of the total flux (0.14–10.0 keV) within the central 3′. Because cooling flow mass deposition rates are inferred from X-ray fluxes, our finding opens the possibility of significantly reducing cooling rates.

Subject headings: cooling flows — X-rays: galaxies — X-rays: galaxies: clusters

1. INTRODUCTION

It is well established that the diffuse X-ray emission from clusters of galaxies implies the existence of a hot (10^7–10^8 K), thermally radiating intracluster medium (ICM). In the dense centers of many clusters this gas is expected to cool radiatively in less than a Hubble time. As pressure support decreases, the gas will gravitate toward the bottom of the cluster potential well, a phenomenon that has come to be known as a "cooling flow" (e.g., Fabian 1994). Such cooling flows can be detected by direct X-ray imaging, where they are seen as a surface brightness enhancement in the X-ray emission from a region typically $\sim$100–200 kpc in radius, and by spectroscopic observations which reveal gas at cooler temperatures than the surrounding ICM. The excess X-ray luminosity in the cooling flow region is typically $10^{42} < L_{\rm cool} < 10^{45}$ ergs s^{-1}, corresponding to roughly 10%–50% of the total cluster X-ray emission (Peres et al. 1998). The mass deposition rate is $\dot{M} \propto L_{\rm cool} T^{-1}$, where T is the gas temperature at $r_{\rm cool}$, the cooling radius. Estimated cooling flow rates in the centers of rich clusters vary from 30 to 300 $M_\odot$ yr^{-1} (White, Jones, & Forman 1997) and in some cases reach mass deposition rates of 1000 $M_\odot$ yr^{-1} or more (Allen 2000).

A long-standing problem with the cooling flow scenario has been the fact that the large quantities of cool gas expected to accumulate from the flow have rarely been detected. Searches for cool gas in atomic or molecular form have generally proven unsuccessful (e.g., Heckman et al. 1989; Jaffe 1990; McNamara, Bregman, & O'Connell 1990; O'Dea et al. 1994; Voit & Donahue 1995; Jaffe & Bremer 1997; Donahue et al. 2000), with reported upper limits 2 orders of magnitude smaller than the masses implied by X-ray mass deposition rates (although see Edge 2001). While some support for the cooling flow picture is provided by low-energy X-ray spectra of clusters which appear to require larger absorption than can be accounted for by foreground gas alone (White et al. 1991; Allen et al. 1993; Irwin & Sarazin 1995), it now appears that the fraction of clusters that actually possess such excess absorption may be much less than previously thought (Arabadjis & Bregman 2000, hereafter AB00; Böhringer et al. 2001b). Furthermore, recent high-resolution X-ray spectra obtained with the *XMM-Newton* and *Chandra* satellites have failed to show expected emission lines from cooled gas at temperatures below a few keV (Fabian et al. 2001; Peterson et al. 2001; Tamura et al. 2001), and it has also been found that local isothermality matches the spectral data of "cooling flow" regions better than the continually declining temperature profile predicted by the standard cooling flow model (e.g., Molendi & Pizzolato 2001; Böhringer et al. 2001b). A variety of mechanisms have been proposed to account for the lack of detectable cool gas in cooling flows; these include reheating the gas, mixing, differential absorption, efficient conversion of cooling flow gas into low-mass stars, inhomogeneous metallicity distributions, or disruption of cooling flows by recent subcluster mergers (see recent discussions in Fabian et al. 2001; Peterson et al. 2001). As of yet, it is unclear whether any of these mechanisms are capable of resolving the aforementioned problems with the cooling flow model.

One characteristic that is common to the mechanisms mentioned above is that they have mainly been introduced in an "after-the-fact" manner. That is, they assume that the observed mass deposition rates are basically correct but that something is happening to the gas after (or while) it cools, be it reheating or conversion into low-mass stars or some other process. Perhaps a simpler way of addressing the problems of the cooling flow model is to look for ways to reduce the mass deposition rates from the beginning. One way to achieve this is to reduce the excess emission ($L_{\rm cool}$) associated with cooling flows by attributing some (or all) of it to X-ray sources other than thermal bremsstrahlung or line emission from the ICM. However, are there sources luminous enough to reproduce $L_{\rm cool}$, can they be found

[1] Department of Astronomy and Physics, Saint Mary's University, Halifax, NS B3H 3C3, Canada.

[2] Current address: Department of Physics and Astronomy, University of Victoria, Victoria, BC V8P 1A1, Canada; mccarthy@beluga.phys.uvic.ca.

[3] Department of Physics and Astronomy, University of Hawaii at Hilo, Hilo, HI 96720.

within galaxy clusters, and, most importantly, can they mimic hot cluster gas?

Soon after X-ray emission was first detected from galaxy clusters, Katz (1976) proposed that much of this emission might come from individual compact sources such as those known to exist in our own Galaxy. However, the subsequent discovery of iron emission lines in X-ray spectra (Forman & Jones 1982 and references therein) clearly demonstrated that thermal bremsstrahlung from a diffuse intracluster gas is the dominant source of X-ray emission in clusters, and interest in compact sources quickly waned. Nevertheless, compact sources must surely contribute some fraction of the total X-ray emission from galaxy clusters. A growing body of evidence indicates that a substantial intergalactic population of stars, star clusters, and stellar remnants is present in the cores of rich clusters, and some of these objects will be X-ray sources. For example, Ferguson, Tanvir, & von Hippel (1998) showed the existence of intergalactic stars in the Virgo Cluster, and planetary nebulae associated with this population have also been detected (e.g., Arnaboldi et al. 1996; Ciardullo et al. 1999). Similarly, West et al. (1995) hypothesized the existence of a large population of intergalactic globular clusters in the cores of galaxy clusters based on observed galaxy-to-galaxy variations in globular cluster populations. Furthermore, there is mounting evidence that many cluster galaxies have been destroyed over a Hubble time, victims of collisions with other galaxies or disruption by the mean tidal field of the cluster potential in which they reside (e.g., Thompson & Gregory 1993; Lopez-Cruz et al. 1997; Gregg & West 1998; Moore et al. 1999; Calcaneo-Rodin et al. 2000). As galaxies are disrupted they will spill their contents throughout intracluster space, including X-ray sources such as X-ray binaries, globular clusters, and black holes. Such disruption is likely to be most frequent in the dense cluster core and hence would be expected to produce a substantial pool of intracluster material, including compact X-ray sources, at the cluster center. Any significant contribution by these compact sources to the X-ray flux will have to be taken into account when estimating the properties of ICM, including temperatures, densities, and cooling flow mass deposition rates.

An intracluster population of compact objects would have a different spectral signature than thermal emission from intracluster gas. For instance, the spectra of large spiral and elliptical galaxies reveal the presence of hard X-ray emission, which is thought to be produced by either high-mass X-ray binaries or accretion onto massive black holes and is adequately represented by power laws having $\Gamma \sim 0.6$–3.0 (where $F_\nu \propto \nu^{-\Gamma}$; Colbert & Mushotzky 1999; Allen, Di Matteo, & Fabian 2000). Luminous active galactic nuclei (AGNs), on the other hand, are often fitted by power laws with $\Gamma \sim 1.6$–2.0 (Nandra et al. 1997). Indeed, the spectral signatures of such objects have already been identified in several X-ray clusters by Allen et al. (2001). Using *ASCA* data, these authors found very luminous sources with power-law spectral indices characteristic of compact sources.

The recent discovery of luminous *extended* nonthermal X-ray emission in several weak (or non–) cooling flow clusters (Rephaeli, Gruber, & Blanco 1999; Fusco-Femiano et al. 1999, 2000, 2001) suggests that one should also look for such emission in massive cooling flow clusters. At present, the origin of the diffuse nonthermal emission is still a matter of some debate. Suggested mechanisms include inverse Compton scattering of cosmic microwave background (CMB) photons up to X-ray energies via a population of highly relativistic electrons, and nonthermal bremsstrahlung, likewise, by a population of relativistic electrons (Sarazin 2001; Rephaeli 2000). Those highly relativistic electrons may have been accelerated by recent subcluster merger events which shocked the ICM or may have been ejected from a central massive black hole. The discovery of X-ray "holes" at the positions of radio lobes of a central compact object in several massive cooling flow clusters (e.g., Böhringer et al. 1993; McNamara et al. 2000; Fabian et al. 2000) certainly lends credence to the second hypothesis. Recently, Harris et al. (2000) (*Chandra* data) and Böhringer et al. (2001a) (*XMM-Newton* data) have even identified extended nonthermal emission directly associated with radio jets/lobes in 3C 295 and M87, respectively.

The spectral signature of extended nonthermal emission is also different from that of thermal emission. To date, the extended nonthermal components of X-ray spectra of clusters have adequately been modeled by power laws having $\Gamma \sim 0.5$–6.0 (Fusco-Femiano et al. 1999, 2000, 2001). As with luminous compact sources, a proper deduction of cluster properties should explicitly include the effects of extended nonthermal emission in the analysis.

In the present work we assess the case for a power-law component to the X-ray spectra of cluster centers, in particular those with cooling flows. We show that simultaneous fits of *ROSAT* Position Sensitive Proportional Counter (PSPC) and *ASCA* Gas Imaging Spectrometer (GIS) and Solid-State Imaging Spectrometer (SIS) spectra, which have been used to infer the presence of cooling flows in many clusters to date, are in fact consistent with a significant contribution from compact sources and/or extended nonthermal emission. Using *ROSAT* High Resolution Imager (HRI) data, we have placed limits on the contribution of any bright point sources within the central regions of these clusters and conclude that the power-law components are most likely produced by either a collection of many low-luminosity compact sources (with $L_X \lesssim 5 \times 10^{42}$ ergs s^{-1}) or diffuse nonthermal emission or some combination of the two. We shall assume $H_0 = 50$ km s^{-1} Mpc^{-1} and $q_0 = 0$ throughout.

2. DATA SELECTION AND REDUCTION

A total of 10 well-studied X-ray luminous galaxy clusters (Table 1) were chosen to span a wide range of cooling flow mass deposition rates. Five of these have essentially no cooling flow (NCF), while the other five cooling flow (CF) clusters have calculated mass deposition rates ranging from 189 to 645 $M_\odot$ yr^{-1}. Observations by the *ROSAT* PSPC and HRI and the *ASCA* GIS and SIS were obtained from the HEASARC public archives and reduced using FTOOLS v5.01. The combination of *ROSAT* and *ASCA* data provides good sensitivity to both soft and hard X-ray emission, spanning the total energy range 0.14–10.0 keV, and should provide a strong test of power-law components in the X-ray spectra of clusters.

2.1. *ROSAT Observations*

The *ROSAT* PSPC data were corrected for spatial and temporal gain fluctuations in the detector. X-ray spectra, spanning the energy range 0.14–2.04 keV, of all 10 clusters were extracted from circular regions centered on the peak of

TABLE 1

CLUSTERS INVESTIGATED IN THIS STUDY

Cluster	z[a]	N_H[b]	Type	$\dot{M}$[c]	kT[d]	Notes
A119	0.0442	3.17	NCF	0	5.3	Three bright radio galaxies near center[e]
A644	0.0704	8.00[f]	CF	189	6.5	Minor merger event[g]
A1689.....	0.1832	1.81	CF	645	8.7	
A2029.....	0.0773	3.14	CF	556	7.4	Nonthermal emission not detected[h]
A2063.....	0.0353	2.90[f]	NCF	37	4.1	Subcluster merger?[i]
A2142.....	0.0909	4.16	CF	350	11.4	Merger[j] and hard X-ray emission detected[k]
A2597.....	0.0852	2.49	CF	271	9.1	Powerful cD radio galaxy[l]
A3266.....	0.0589	3.00[f]	NCF	0	6.2	Major merger[m]
A3532.....	0.0554	5.98	NCF	0	4.7	Merger[n]
A3667.....	0.0556	4.00[f]	NCF	0	7.1	Hard X-ray emission found[o]

[a] Redshifts from the NASA/IPAC Extragalactic Database.
[b] Galactic H I column density (in units of 10^{20} cm^{-2}) from Dickey & Lockman 1990, except where noted.
[c] Mass deposition rate (in $M_\odot$ yr^{-1}) from Peres et al. 1998.
[d] Single-phase ICM temperature (in keV) reported by White et al. 1997.
[e] Feretti et al. 1999.
[f] Galactic H I column density (in units of 10^{20} cm^{-2}) from Stark et al. 1992.
[g] Bauer & Sarazin 2000.
[h] Molendi & De Grandi 1999.
[i] Oegerle & Hill 1994.
[j] Markevitch et al. 2000.
[k] Bazzano et al. 1984.
[l] Sarazin et al. 1995.
[m] Flores, Quintana, & Way 2000.
[n] Bardelli, Zucca, & Baldi 2001.
[o] Fusco-Femiano et al. 2001.

the emission with a constant extraction radius (R) of 3′. Background spectra were selected from source-free circular regions of radius R. All spectra were corrected for the effects of cosmic rays in the detector (Snowden et al. 1992), vignetting, spatial variations in detector efficiency, and dead time. The background-subtracted spectra were then grouped to ensure a minimum of 20 counts per radial bin so that reliable χ^2 statistics could be computed.

The *ROSAT* HRI data were reduced in a manner similar to the PSPC data. The HRI data were used to place limits on the contribution of any point sources within the central regions of these clusters. Unfortunately, the HRI lacks spectral resolution and was not used in the main spectral analysis. A description of the analysis of HRI data is given in § 5. No HRI data were available for A2063 or A3532.

2.2. *ASCA Observations*

The screened events from "revision 2" processing of *ASCA* GIS/SIS data were used. Additional cleaning procedures (discussed in the *ASCA* ABC Guide) were implemented, including gain and dead-time corrections. For the GIS detectors (GIS2 and GIS3), X-ray spectra spanning the energy range 0.7–10.0 keV were extracted from the same region of sky as that of the *ROSAT* PSPC source spectra. For the SIS detectors (SIS0 and SIS1), X-ray spectra spanning the range 2.0–10.0 keV were extracted, thus avoiding complications with the degrading efficiency of the SIS detectors at low energies. Background spectra for both the SIS and GIS detectors were extracted from the "blank sky" observations made during the performance testing stage of the mission. Spectra were extracted from the same regions of the detectors as that of the source spectra (thus minimizing position-dependent effects associated with background subtraction). The background-subtracted spectra were also grouped (or binned) to ensure that χ^2 statistics could be used. For the clusters A2142 and A3667 SIS1 data were ignored because of an excess of hot and flickering pixels.

3. SPECTRAL ANALYSIS

Reduced *ROSAT* PSPC and *ASCA* GIS/SIS spectra were fitted simultaneously using models within the software package XSPEC v11 (Arnaud 1996). Each cluster was fitted with a variety of models based on the MEKAL thermal plasma routine (Mewe, Gronenschild, & van den Oord 1985; Kaastra 1992; Liedahl, Osterheld, & Goldstein 1995) and/or redshifted power laws. In addition, we used the popular cooling flow model comprising a thermal plasma (MEKAL) and cooling flow component implemented by the MKCFLOW routine within XSPEC (Mushotzky & Szymkowiak 1988). Fits were obtained by varying the temperature (kT) and metallicity (Z) of the thermal plasma component(s) and by varying the photon index (Γ) of any power-law components. Photoelectric absorption (Balucinska-Church & McCammon 1992) was applied to the spectral models through two separate methods: (1) by applying only one absorption component to the entire spectral model and fixing the H I column density (N_H) at the known Galactic value (see Table 1) and then letting it vary to see if the fit could be improved, and (2) by applying one absorption component to the entire spectral model (with N_H fixed at the Galactic value) and a separate redshifted variable absorption component ($N_{H,PL}$) to any power-law components via the ZPHABS model in XSPEC. The second method allows for *intrinsic* absorption to be associated with any power-law components. Spectra of nearby high-mass X-ray binaries and accreting massive black holes provide strong evidence for heavy intrinsic absorption, with $N_H \sim 10^{21}$–10^{23} cm^{-2} above the Galactic column (Colbert & Mushotzky 1999; Iwasawa et al. 2000; Akylas, Georgantopoulos, & Comastri 2001). We therefore regard the

addition of a free intrinsic absorption parameter as an important feature of our spectral analysis.

Henceforth we will use TP, PL, and CF to refer, respectively, to thermal plasma (MEKAL), power-law, and MKCFLOW components. For example, in this notation TPPL identifies a model having thermal plasma and power-law components. Goodness of fit was judged by the reduced χ^2 (χ_r^2) and by visual inspection of residual plots. When additional components were added to a spectral model, for example, adding a power-law component to a thermal plasma component to make TPPL, the corresponding F-statistic was calculated in order to judge whether the addition was reasonable. Unless stated otherwise, the derived relative contributions of each of the components to the total flux refer to the energy range 0.14–10.0 keV stated, whereas the luminosities presented refer to the *ASCA* GIS band only (0.7–10.0 keV), since the spectra were fitted simultaneously and not combined. All luminosities presented were corrected for Galactic absorption only.

To check our data reduction procedures, spectra from each of the detectors were also fitted individually and no significant deviations were found. We have also attempted to duplicate published results by AB00 for three clusters derived using the same data (*ROSAT* PSPC) and the same software. The results, which refer to the inner 3′ radius, are presented in Table 2. Here the hotter TP component is fixed at the White et al. (1997) value, $Z = 0.5\ Z_\odot$; $N_{\rm H}$ is fixed at the Stark et al. (1992) value; and the energy range is 0.14–2.4 keV and 0.14–2.04 keV for AB00 and our study, respectively. The comparison shows excellent agreement, with derived temperatures and mass deposition rates having the same values to within 1 σ.

4. RESULTS

4.1. *Non–Cooling Flow Clusters*

We find that single-temperature TP models provide acceptable fits to the spectra of A119, A2063, A3266, A3532, and A3667 ($1.00 \leq \chi_r^2 \leq 1.17$) with temperatures in very good agreement with previous studies (White et al. 1997; Markevitch et al. 1998). Significant improvement is not usually obtained by varying the hydrogen column density from the known Galactic value reported by Dickey & Lockman (1990) or Stark et al. (1992). The derived metallicities range from $0.2 \lesssim Z \lesssim 0.4$, which is typical of the ICM (Allen & Fabian 1997).

In general, both pure PL models with or without variable intrinsic absorption do not provide acceptable fits to the NCF cluster spectra with $\chi_r^2 \gtrsim 1.4$. This result is not unexpected since it leaves no room for thermal emission from the ICM. With intrinsic absorption included, an acceptable fit is obtained for A3532 with $\chi_r^2 \approx 1.05$, however. This cluster is located at the center of the Shapley Concentration and is thought to be undergoing a merger with A3528. The diffuse nonthermal emission generated from such a merger might possibly account for the ability of the simple PL model to fit the spectrum of A3532. Unfortunately, no HRI data exist for this cluster, so we cannot place limits on the contribution of any point sources within the central 3′.

In the best-fitting TPPL models, the PL component typically contributes 1%–14% (mean of 7%) when absorbed by the Galactic column only or 10%–25% (mean of 20%) when intrinsic absorption is included (excluding A3532, which has an anomalously large PL component). We note that in virtually every case the inclusion of intrinsic absorption noticeably improves the quality of the fit, making it superior to even the simple TP models (see Table 3). A mean F-statistic of ≈ 10 ($\gtrsim 95\%$ confidence) was found when the PL component with intrinsic absorption was included in the fit, indicating that its addition is, indeed, reasonable. The corresponding luminosities of intrinsically absorbed PL components range from $L_{\rm X,0.7-10.0} \approx 5 \times 10^{42}$ to 7×10^{43} ergs s^{-1} with a mean value of $L_{\rm X,0.7-10.0} \approx 2.2 \times 10^{43}$ ergs s^{-1} (corrected for Galactic absorption only). Photon indices for these components are typical of compact accretion-driven X-ray sources and extended nonthermal emission. Interestingly enough, the amount of intrinsic absorption ranges from $1.8 \times 10^{21} \leq N_{\rm H,PL} \leq 1.4 \times 10^{22}$ cm^{-2}, which is typical of optically thick compact sources. We also note that the temperature of the ICM tends to decrease significantly when a power-law component is included. This trend was previously reported by Allen et al. (2001) when including a power-law component in their spectral models. Figure 1 presents the best-fit TPPL model to the spectrum of A3667. For clarity, only the *ROSAT* PSPC data are plotted.

As expected, standard cooling flow (TPCF) models of our non–cooling flow sample yield best fits with $\dot{M} = 0\ M_\odot$ yr^{-1} to within 1 σ. The mass deposition rate for the modest cooling flow cluster A2063, however, is $25 \pm 12\ M_\odot$ yr^{-1}. The cooler component in our TPTP models typically contributes zero flux to within 1 σ ($\sim 10\%$ for A2063 and A3667). Neither of these models provided fits significantly better than those of the standard TP models.

In summary, we confirm earlier investigations which find that TP models provide satisfactory fits to *ROSAT* and *ASCA* spectra of the centers of non–cooling flow clusters. However, TPPL models which include intrinsic absorption generally provide fits of superior quality and predict that the power-law component contributes 20% of the total flux. The photon indices of this component are typical of accret-

TABLE 2

COMPARISON WITH AB00

Cluster	Model	$kT_{\rm cool}$[a]	$\dot{M}$[b]	χ_r^2	$kT_{\rm cool}$[c]	$\dot{M}$[d]	χ_r^2
A119	TP	...	...	0.987	...	...	1.011
	TPCF	$0.08 \pm \infty$	0 ± 3	0.994	0.01 ± 151	0.6 ± 5	1.026
A2029	TPTP	1.29 ± 0.15	...	1.592	1.19 ± 0.31	...	1.499
	TPCF	0.08 ± 6.97	132 ± 31	1.911	0.03 ± 4.82	170 ± 43	1.772
A2142	TPCF	0.08 ± 7.41	188 ± 43	1.190	0.10 ± 9.16	230 ± 73	1.130

[a] Temperature (in keV) of the cooler TP component found by AB00.
[b] Mass deposition rate (in $M_\odot$ yr^{-1}) found by AB00.
[c] Temperature (in keV) of the cooler TP component found in this study.
[d] Mass deposition rate (in $M_\odot$ yr^{-1}) found in this study.

TABLE 3

COMPARISON OF THE TP AND TPPL MODELS FOR THE NCF CLUSTERS

Cluster	Model	kT[a]	Γ[b]	PL[c] (%)	$N_{H,PL}$[d]	χ^2/dof
A119	TP	5.91 ± 0.20	...	...	...	467.4/446
	TPPL	3.96 ± 0.78	1.55 ± 0.17	25	29.5 ± 17.6	454.0/443
A2063.....	TP	3.09 ± 0.05	...	...	...	945.6/807
	TPPL	2.49 ± 0.23	1.41 ± 0.27	8.5	47.5 ± 71.5	933.3/804
A3266.....	TP	8.48 ± 0.24	...	...	...	1160.5/1117
	TPPL	4.23 ± 0.86	1.33 ± 0.12	23	140.0 ± 35.2	1158.0/1114
A3532.....	TP	4.55 ± 0.13	...	...	...	776.4/746
	TPPL	3.71 ± 1.14	2.12 ± 0.10	87.5	18.0 ± 2.70	756.0/743
A3667.....	TP	5.64 ± 0.14	...	...	...	809.0/791
	TPPL	3.22 ± 0.32	1.30 ± 0.15	22	88.0 ± 40.4	797.6/788

[a] Temperature (in keV) of the thermal plasma component.
[b] Photon index of the power-law component.
[c] Contribution of the PL component to the total flux (0.14–10.0 keV).
[d] Intrinsic H I column density (in units of 10^{20} cm^{-2}) acting on the PL component.

ing X-ray sources and/or diffuse nonthermal X-ray emission, which usually range from $1.0 \lesssim \Gamma \lesssim 3.0$.

4.2. *Cooling Flow Clusters*

We have fitted the spectra of the CF clusters with the same variety of models used in the previous section, but also with an additional model: TPTPPL. This model represents the emission from the observed region as the sum of the hot ICM, a diminished cooling flow (second TP component), and intermixed compact sources and/or extended nonthermal emission characterized by the PL component.

Simple TP models generally provide fairly reasonable fits to the spectra with $1.1 \lesssim \chi_r^2 \lesssim 1.25$. Derived temperatures and metallicities are in good agreement with previous studies (White et al. 1997; Allen & Fabian 1997; Sarazin & McNamara 1997; Markevitch et al. 1998; Allen 2000; AB00; Allen et al. 2001). None of the fits were significantly improved by letting the value of N_H vary. Hence, we find no evidence for excess absorption in these clusters, which is also consistent with several other investigations (Sarazin 1996; Allen & Fabian 1997; Sarazin & McNamara 1997; Allen 2000; AB00).

As anticipated, pure PL models (with or without intrinsic absorption) do not provide acceptable fits to the X-ray spectra of any of the CF clusters. Typically, $\chi_r^2 \gtrsim 1.5$ for this model.

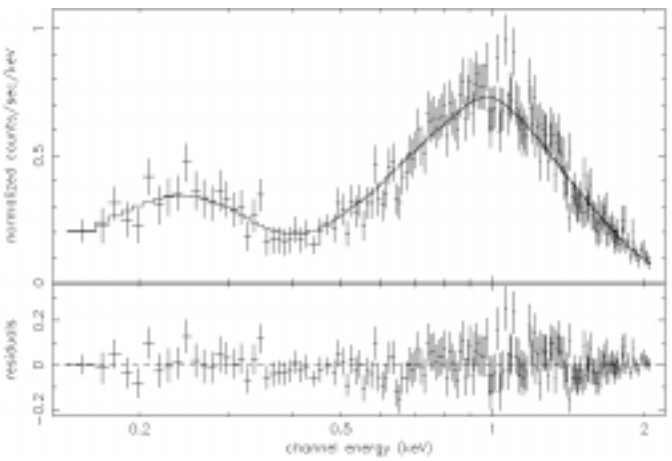

FIG. 1.—Best-fitting TPPL model on the spectrum of A3667. The power-law component has a photon index of 1.30 and contributes ≈22% of the flux over the range 0.14–10.0 keV. Only the *ROSAT* PSPC data are presented here.

Our TPPL models fit the spectra of all five CF clusters very well, with $1.0 \lesssim \chi_r^2 \lesssim 1.2$ (see Table 4). With the exception of A2029, which is best fitted by simple TP models, the PL component typically contributes 5%–30% (mean of 20%) of the total flux when absorbed only by the Galactic column. The inclusion of intrinsic absorption significantly improves the quality of the fit and raises the contribution of the PL component to 9%–47% (mean of 27%). The mean F-statistic value for the addition of this power-law component is ≈50, which suggests that it is significant (greater than 99% confidence). The luminosities (0.7–10.0 keV) of PL components in these four clusters span $\approx 0.9\text{–}8 \times 10^{44}$ ergs s^{-1}, with a mean value of $\approx 3.8 \times 10^{44}$ ergs s^{-1}. The photon indices of PL components are reasonably well constrained and range from $1.0 \lesssim \Gamma \lesssim 2.4$ (mean of 1.8) (see Table 4). The implied intrinsic column densities acting on the PL component are rather high for three of the CF clusters (A644, A1689, and A2597) and are consistent with high-mass compact sources. As with the NCF clusters, a lower temperature is found for the thermal component than is found from the simple TP models.

TPTP models were also implemented. The quality of the fits provided by these models is generally comparable to that of TPPL models. Calculation of the F-statistic suggests that the addition of the extra TP component is significant. Thus, we confirm previous reports that multiphase thermal plasmas fit the spectra of CF clusters much better than that of isothermal models. The temperatures and metallicities of the two thermal components are consistent with the results of previous studies (White et al. 1997; Markevitch et al. 1998; Allen 2000; AB00; Allen et al. 2001). For the cooler component in particular, we find $1.4 \lesssim kT \lesssim 2.2$ and a mean contribution of roughly 22% of the total flux, which is typical of cooling flow clusters (Peres et al. 1998).

The standard cooling flow model (TPCF) provides adequate fits to the spectra of the CF clusters, as expected. Derived mass deposition rates, temperatures, and metallicities are generally consistent with previous studies (White et al. 1997; Peres et al. 1998; Allen et al. 2001; Allen 2000; AB00). The best-fitting TPCF model to the spectrum of A644 is presented in Figure 2. Only the *ASCA* SIS0 and GIS2 data are plotted. A comparison of the TPCF and TPPL models is presented in Table 4. It is clear that the

TABLE 4

COMPARISON OF THE TPPL AND TPCF MODELS FOR THE CF CLUSTERS

Cluster	Model	$\dot{M}$[a]	Γ[b]	PL[c] (%)	$N_{H,PL}$[d]	χ^2/dof
A644	TPPL	...	2.37 ± 0.78	35	24.1 ± 20.6	1855.7/1613
	TPCF	200 ± 71	...	...	...	1841.2/1613
A1689.....	TPPL	...	1.02 ± 0.29	9	166.0 ± 71.5	1643.6/1409
	TPCF	504 ± 149	...	...	...	1653.9/1409
A2029.....	TPPL	...	2.13 ± 1.44	5	3.34 ± 6.40	1460.3/1149
	TPCF	427 ± 60	...	...	...	1462.1/1149
A2142.....	TPPL	...	1.67 ± 0.09	47	2.14 ± 0.54	1010.4/868
	TPCF	307 ± 90	...	...	...	1013.2/868
A2597.....	TPPL	...	1.89 ± 0.45	17	177.0 ± 72.0	1305.1/1281
	TPCF	217 ± 23	...	...	...	1302.3/1281

[a] Mass deposition rate (in $M_\odot$ yr^{-1}).
[b] Photon index of the power-law component.
[c] Contribution of the PL component to the total flux (0.14–10.0 keV).
[d] Intrinsic H I column density (in units of 10^{20} cm^{-2}) acting on the PL component.

TPPL models fit the spectra of the five CF clusters just as well as standard TPCF models and without any additional complexity.

Finally, the TPTPPL model also fits the X-ray spectra of these clusters well, with $1.0 \lesssim \chi^2_r \lesssim 1.2$. When absorbed by the Galactic column only, the PL component typically contributes 2%–5% of the total flux inside 3′. The addition of intrinsic absorption on the PL component, again, improves the fit, and the mean contribution of the PL component is raised to $\approx$32%. When compared to the TPPL model, the mean F-statistic value is about 5 ($\approx$68% confidence), which suggests that the addition of a second TP component only improves the fit marginally. The luminosity (0.7–10.0 keV) of the PL component is in the range $1–6 \times 10^{44}$ ergs s^{-1} with a mean value of $\approx 2.2 \times 10^{44}$ ergs s^{-1}. The power-law components have photon indices of $1.8 \lesssim \Gamma \lesssim 3.3$ with a mean of 2.3. With the exception of A2029 (which has virtually no contribution from the PL component), the intrinsic column densities on the PL component are $\gtrsim 10^{21}$ cm^{-2}. The temperature of the cooler TP component did not change significantly from the value derived from TPTP models. However, its contribution to the flux was generally lower than that of TPTP models (mean $\sim$10%).

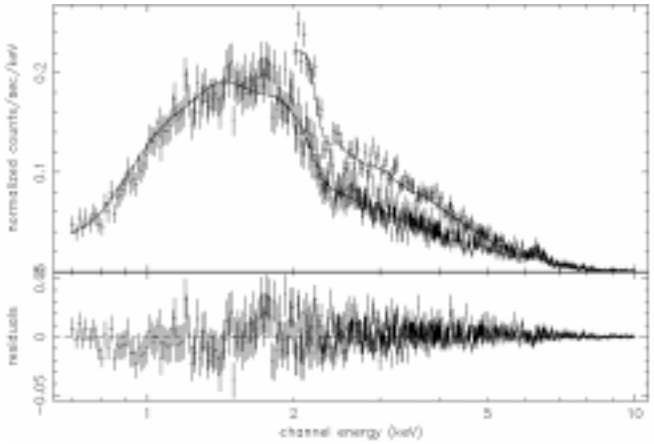

FIG. 2.—*ASCA* SIS0 and GIS2 spectra of the CF cluster A644. The SIS0 spectrum ranges from 2.0 to 10.0 keV, while the GIS2 spectrum ranges from 0.7 to 10.0 keV. Both data sets are shown in the residuals in the bottom part of the plot. The best-fitting TPCF model predicts a mass deposition rate of 200 $M_\odot$ yr^{-1}.

In summary, we find that in all cases the TPPL and TPTPPL models fit the *ROSAT* and *ASCA* spectra of the five CF clusters just as well as the standard cooling flow model (TPCF) or the two-temperature thermal plasma (TPTP). The PL components of these models are quite luminous (contributing between 27% and 32% of the total flux) and characterized by photon indices typical of compact accreting X-ray sources and/or extended nonthermal emission. This, then, is the main conclusion of our work: *ROSAT and ASCA spectra can be satisfactorily modeled by attributing a significant part of the luminosity within the central regions of CF clusters to sources other than cooling gas.*

5. DISCUSSION

Our analysis shows that luminous ($L_{X,0.7-10.0} \sim 10^{42}$–$10^{44}$ ergs s^{-1}) power-law components with $1.0 \lesssim \Gamma \lesssim 3.0$ might be present in the centers of rich clusters. Including intrinsic absorption dramatically improves the quality of the fit; in these circumstances, there is an apparent dichotomy in the importance of the PL components between NCF and CF clusters. Not only is the typical PL component in the CF cluster more luminous by about a factor of 10 than that of its NCF counterpart, but it also contributes a larger fraction of the total X-ray flux within the central 3′ of its cluster (between 27% and 32% for CF clusters as opposed to 20% for NCF clusters). This may be consistent with the fact that the *cores* of CF clusters are more often observed to be active (i.e., radio-loud), perhaps implying the presence of a central massive black hole(s) and a surrounding diffuse plasma of relativistic electrons, than the cores of NCF clusters (Burns 1990). It is also worth noting that the improvement of the fit to the spectra of CF clusters far exceeds the improvement of the fit to the spectra of NCF clusters when a power-law component is included in the spectral model.

The most attractive feature of the TPPL models is that one does not expect large quantities of atomic or molecular gas to be present in the centers of clusters, nor does one expect to see emission lines below a few keV, because cooling is not significant. This is consistent with current observations. On the other hand, evidence which apparently supports the existence of cooling flows (e.g., excess absorption, detection of CO line emission in extreme CF clusters) may contradict this model. However, the success of

the single-temperature plasma plus power-law model in fitting the spectra of the central regions of rich clusters, regardless of cooling flow status, has also been reported by a number of authors using a variety of X-ray instruments, including Markevitch & Vikhlinin (1997) (*ASCA* and *ROSAT* data), Markevitch et al. (1998) (*ASCA* data), Rephaeli et al. (1999) (*RXTE* data), Guainazzi & Molendi (1999) (*BeppoSAX* data), Fusco-Femiano et al. (1999, 2000, 2001) (*BeppoSAX* data), and recently Sambruna et al. (2000), who used *Chandra* to uncover a previously *hidden* AGN in Hydra A with $L_{X,2-10} \gtrsim 10^{42}$ ergs s^{-1} and $\Gamma \sim 1.7$. However, our study is the first that systematically addresses the problems of the standard cooling flow model by implementing the single-temperature plasma plus power-law model.

The TPTPPL models, which might represent a compromise between the standard cooling flow model and our favored TPPL models, also provide good fits to the spectra of the CF clusters. However, the addition of the second, cooler TP component only marginally improves the fit and at the expense of adding much more complexity (and uncertainty) to the model. Furthermore, the predicted temperatures and relative contributions of the cooler TP component in the TPTPPL models suggest that emission lines below a few keV should be present; however, they have failed to turn up in *Chandra* and *XMM* spectra. Finally, because the mean contribution of the cooler component is $\sim$10%, as compared with 20% in the TPTP models, this implies that mass deposition rates are only roughly reduced by a factor of 2. Using models similar to our TPTPPL models, Allen et al. (2001) reached the same conclusion for a number of clusters in their sample. These reduced deposition rates are still far too large to be consistent with the small amounts of atomic and molecular gas found in cooling flow clusters. We expect that *Chandra* and *XMM-Newton* will place much tighter constraints on the parameters of the complex TPTPPL models, and it will be interesting to see if the models can be reconciled with problems of the standard cooling flow model.

Assuming that a power-law component is, indeed, present in the spectra of these clusters, some of the possible candidates are as follows:

1. Seyfert-like AGNs could contribute most, if not all, of the PL component luminosity found in our study. These objects can be quite luminous and are often observed to have $L_X \sim 10^{41}$–10^{44} ergs s^{-1} with power-law indices of 1.6–2.0 (Nandra et al. 1997). In fact, Allen et al. (2001) have suggested that AGNs are the likely candidate for the observed PL component in their sample. Likewise, the luminosities and steepness of the PL components in our sample are generally consistent with emission from a central AGN(s).

2. Diffuse nonthermal emission, which has possibly been seen in the central regions of Coma, A2256, and A2199. Searches of those clusters using *BeppoSAX* and *RXTE* have yielded very luminous ($\approx 10^{42}$–10^{44} ergs s^{-1}) sources which are described by power laws with $\Gamma \sim 0.5$–6 and may possibly be linked to power-law components observed in the *ASCA* band (Rephaeli et al. 1999; Fusco-Femiano et al. 1999, 2000, 2001). Unfortunately, X-ray spectra usually have to be extracted from regions *much* larger than that of the central galaxy, and thus it is difficult to draw conclusions about the source of the power-law component. A VLA survey of more than 200 nearby clusters found that only 29 had extended radio emission on megaparsec scales (Giovannini, Tordi, & Feretti 1999), perhaps implying that extended nonthermal emission is not that common in galaxy clusters. It should be noted, however, that the detection of true intracluster radio emission is exceptionally difficult, as one must remove bright radio galaxies from the analysis (Rephaeli 2000). Furthermore, the nonthermal emission may be associated with the radio galaxies themselves (e.g., in the radio lobes).

3. Massive black holes associated with elliptical and lenticular galaxies. The regions sampled in our study generally include a single giant elliptical or cD galaxy plus a number of large galaxies, probably E or S0 galaxies. Colbert & Mushotzky (1999) and Allen et al. (2000) have recently discovered hard power-law components in several nearby gE galaxies with $10^{37} \lesssim L_X \lesssim 10^{42}$ ergs s^{-1} with photon indices of 0.5–3.0. Such sources are typically less luminous than Seyfert nuclei, perhaps as a result of low radiative efficiency from an advection-dominated accretion flow (ADAF; Narayan & Yi 1995). While several of these sources could, in principle, account for the PL component in the NCF clusters, they would have to be scaled up by a factor of 100 to account for the emission in the CF clusters. Faint galaxies, on the other hand, are much more numerous, and many of them might harbor less massive central black holes. The Local Group elliptical M32, whose central object has $L_X \sim 10^{37}$ ergs s^{-1} (Loewenstein et al. 1998), offers a possible guide to the X-ray luminosity of faint cluster members. Hence, $\sim 10^4$–10^6 such galaxies, each with a supermassive black hole, would be required to account for the power-law component of the clusters studied here. On this basis, faint galaxies seem incapable of producing significant power-law emission inside the regions we have observed. We note, however, that if massive black holes originally belonging to bright or faint galaxies are now scattered throughout intracluster space (i.e., no longer associated with optically visible galaxies) as the result of past mergers or stripping, both of these limits may be relaxed.

4. Galactic X-ray binaries, having $\Gamma \approx 0$–2.5 (White, Stella, & Parmar 1988; Verbunt et al. 1995), and which in our galaxy are most commonly associated with globular clusters. Intergalactic globular clusters, if similar to globular clusters in the Milky Way, would have to be present in large numbers to collectively account for $\sim 10^{42}$–10^{44} ergs s^{-1} attributable to the PL component in our models. Assuming that a typical intergalactic globular contains a binary X-ray source with $L_X \sim 10^{35}$ ergs s^{-1} (Hertz & Wood 1985) and that the specific frequency of globulars in the central gE galaxy is $S_N = 10$ (Harris 1991), then even a very bright central galaxy with $M_B = -24$ would have a total X-ray luminosity of $\sim 10^{39}$ ergs s^{-1}, too low by a factor of 10^4–10^5. Even the most optimistic models of intracluster globular clusters of West et al. (1995) predict $\sim 10^4$–10^5 such clusters, significantly less than is required to account for the entire PL component.

Hence, it appears that there are probably two or three sources capable of producing the luminosity of the PL components of our models: massive black holes associated (or once associated) with large elliptical galaxies, diffuse nonthermal emission, and AGNs. Do existing data favor one type of source over the others?

To determine the luminosity of any point sources within

the central 3′, we used *ROSAT* HRI data. Two different procedures were implemented. (1) Spectra of clearly visible point sources were extracted from a 5″ region centered on the source and grouped into one large energy bin (0.5–2.0 keV). The spectra were then fitted within the XSPEC package using a simple power-law model with $\Gamma = 1.8$ and absorbed by the Galactic column only. The 0.5–2.0 keV flux was then converted into a 0.7–10.0 keV unabsorbed flux using the program W3PIMMS. If more than one point source was present, the individual fluxes were summed. As an example, Figure 3 is the HRI observation of A3667, smoothed with a 5″ Gaussian beam. There are at least two bright compact sources within the central 3′ of this cluster. (2) To place limits on the contribution of point sources which are hidden in the bright diffuse background (what we refer to as "barely visible" point sources), we calculated the mean standard deviation of counts per pixel (within 3′) and then scaled this to a standard deviation per circular region of diameter equal to 5″ (comparable to the HRI point-spread function). The latter value was expressed as unabsorbed flux (0.7–10.0 keV) using the program W3PIMMS and assuming a simple power-law spectral model with $\Gamma = 1.8$ absorbed only by the Galactic column listed in Table 1. We regard the result as a 1 σ limit to the contribution of any point sources.

The results of HRI data analysis are presented in Table 5.

TABLE 5

LIMITS IN cgs UNITS ON POINT-SOURCE CONTRIBUTION FROM HRI DATA

Cluster	Method I[a]	Method II[b]	$L_{X,PL}$[c]
A119	8.12×10^{41}	$\leq 5.40 \times 10^{40}$	$1.67^{+1.46}_{-0.97} \times 10^{43}$
A644	...	$\leq 2.99 \times 10^{41}$	$2.59^{+2.74}_{-1.42} \times 10^{44}$
A1689.....	...	$\leq 2.09 \times 10^{42}$	$2.95^{+4.70}_{-2.95} \times 10^{44}$
A2029.....	...	$\leq 5.34 \times 10^{41}$	$8.65^{+31.68}_{-8.65} \times 10^{43}$
A2142.....	...	$\leq 6.45 \times 10^{41}$	$8.81^{+4.22}_{-2.95} \times 10^{44}$
A2597.....	...	$\leq 7.02 \times 10^{41}$	$0.94^{+2.37}_{-0.94} \times 10^{44}$
A3266.....	1.47×10^{42}	$\leq 8.40 \times 10^{40}$	$6.28^{+7.91}_{-5.11} \times 10^{43}$
A3667.....	8.01×10^{42}	$\leq 8.97 \times 10^{40}$	$5.70^{+5.46}_{-3.89} \times 10^{43}$

[a] Luminosity of visible point sources.

[b] Upper limit of luminosity of "barely visible" point sources within the HRI point-spread function.

[c] Luminosity of the PL component of the best-fitting TPPL models with intrinsic absorption.

One or more point sources are easily visible within the central 3′ of all three NCF clusters having HRI observations. It is clear from a comparison with the luminosities of the observed PL component from the best-fitting TPPL models (with intrinsic absorption), however, that the bright point sources cannot be solely responsible for the power-law emission, as they contribute only $\approx 5\%$ of the PL com-

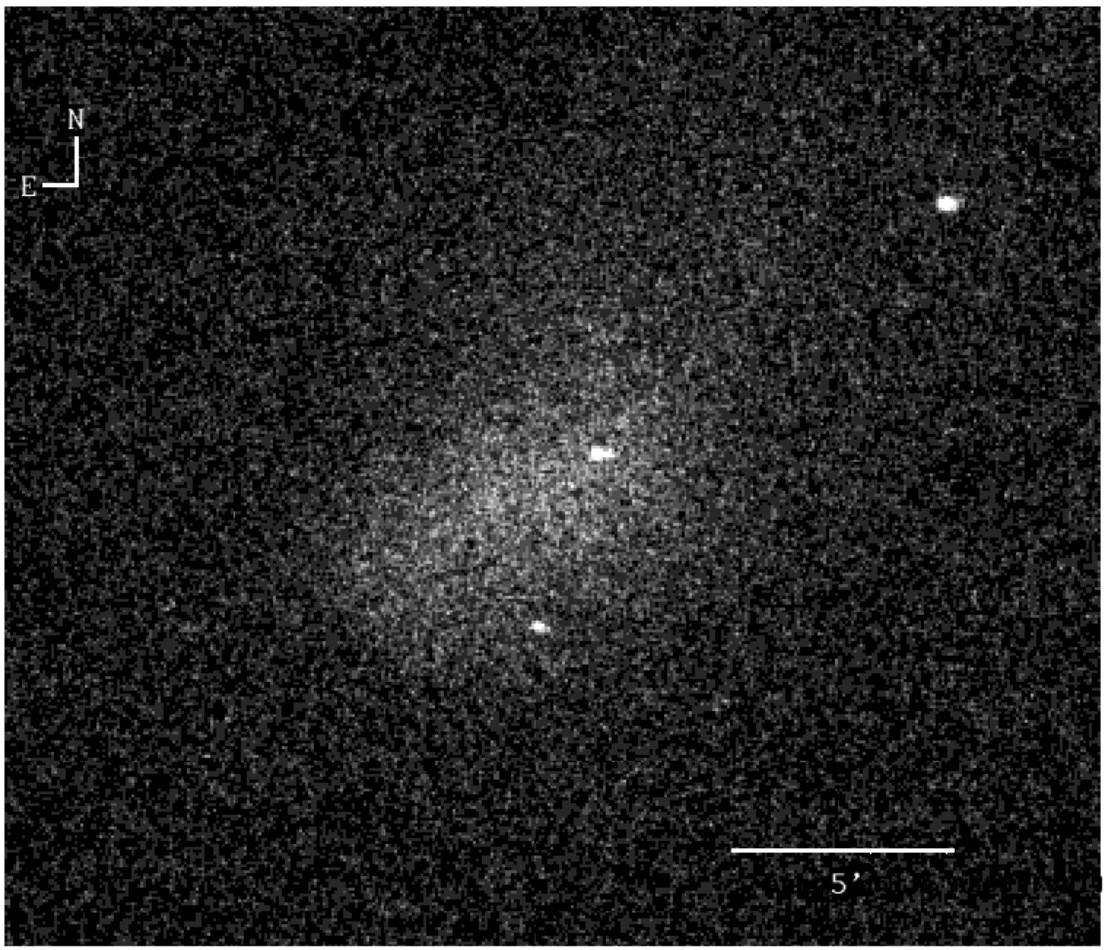

FIG. 3.—*ROSAT* HRI observation of A3667 (centered on R.A. $20^h12^m31^s$, decl. $-56°49'12''$, J2000.0). Two extremely bright compact sources are visible within the central 3′ but together are roughly a factor of 7 less luminous than the spectrally determined power-law component in the best-fitting TPPL model.

ponent luminosity. Significant contributions are required from low-luminosity point sources and/or diffuse nonthermal emission. The third column in Table 5 (Method II) presents the 3 σ limit of "barely visible" point sources, suggesting that at least 10^2–10^3 of them are needed (in addition to the visible point sources) to account for the entire power-law component.

There are no visible point sources within the central 3′ of the five CF clusters studied. This is almost certainly the result of the CF clusters being much more centrally peaked than the NCF clusters. At least 10^2–10^3 "barely visible" point sources are required to account for the observed PL component in these clusters.

Perhaps another way to differentiate between compact sources and diffuse nonthermal emission is through the presence or absence of flux variability, since most luminous accreting X-ray sources are known to vary significantly on short timescales (e.g., Nandra et al. 1997). However, because the PL component typically contributes only $\approx 20\%$, this might make detection of variability difficult in clusters (especially in the CF clusters). Furthermore, if the PL component is produced by 10^2–10^3 point sources, and the variations in each are random, it will make the variation in the collective luminosity quite small, perhaps rendering this method unusable.

If compact or diffuse nonthermal sources provide significant emission from the centers of rich clusters, it will be necessary to revise a number of conclusions derived from X-ray data. Fully exploring the consequences is beyond the scope of the present paper; however, we will mention a few important issues. Allen (2000) reports that a deprojection analysis of *ROSAT* HRI data yields cooling flow mass deposition rates that agree reasonably well with those derived from *ASCA* spectra. A consistent reanalysis would require first subtracting the power-law contribution from the X-ray images, but of course the spatial distribution of the power-law emission must first be understood. The presence of emission lines from heavy ions originally led astronomers to accept thermal emission as the dominant mechanism in rich cluster ICMs. Accretion-driven X-ray sources do exhibit line emission (Kallman, Vrtilek, & Kahn 1989; Narayan & Raymond 1999), but the lines are produced under quite different physical conditions than those within the canonical hot ICM. The implications for ICM abundance estimates and enrichment scenarios will require careful study. Likewise, previously derived temperatures of the ICM will also be affected (as demonstrated in Table 3). Might emission from compact sources account for the excess hard X-radiation recently discovered (Xu et al. 1998; Ikebe et al. 1997) in the centers of several clusters? The next generation of X-ray detectors and satellites (i.e., *XMM* and *Chandra*) will be needed to map the X-ray emission with adequate spatial resolution to address this and other questions raised by the present work.

6. CONCLUSIONS

We have shown that *ROSAT* PSPC and *ASCA* GIS2/GIS3 spectra of 10 X-ray luminous clusters permit a significant contribution from compact sources and/or diffuse nonthermal emission. Although this conclusion holds irrespective of the presence of a cooling flow, we find that power-law components are especially luminous in clusters with massive cooling flows. Our study indicates that inferred cooling flow mass deposition rates may be lowered substantially, thus ameliorating, or possibly resolving, the long-standing problem of the missing cool gas. Existing X-ray observations of large elliptical galaxies, AGNs, and extended nonthermal emission suggest that any of these sources could account for the observed luminosity of the power-law component. However, the absence of extremely bright point sources in the *ROSAT* HRI observations rules out the possibility that the power-law emission comes from a few extremely bright compact sources. It is more likely that most of the power-law emission is produced by some combination of diffuse and low-luminosity compact sources, such as massive black holes. The deep imaging capabilities and superior spectral resolution of *Chandra* and *XMM* should be able to place much tighter constraints on the relative contributions of power-law sources and thermal bremsstrahlung to cluster X-ray emission and, perhaps, even determine the source of the power-law emission.

We thank the *ROSAT* and *ASCA* help teams, in particular Jane Turner, for advice with data reduction techniques. We also thank Paul Nandra, Peter Thomas, Arif Babul, Ann Gower, Pat Henry, and Alastair Edge for useful comments and suggestions. I. G. M. acknowledges support from NSERC of Canada (USRA and PGSA). G. A. W. and M. J. W. were supported by NSERC research grants. M. J. W. also acknowledges support from NSF grant AST-0071149.

REFERENCES

Akylas, A., Georgantopoulos, I., & Comastri, A. 2001, MNRAS, 324, 521
Allen, S. W. 2000, MNRAS, 315, 269
Allen, S. W., Di Matteo, T., & Fabian, A. C. 2000, MNRAS, 311, 493
Allen, S. W., et al. 1993, MNRAS, 262, 901
———. 2001, MNRAS, 322, 589
Allen, S. W., & Fabian, A. C. 1997, MNRAS, 286, 583
Arabadjis, J. S., & Bregman, J. N. 2000, ApJ, 536, 144 (AB00)
Arnaboldi, M., et al. 1996, ApJ, 472, 145
Arnaud, K. A. 1996, in ASP Conf. Ser. 101, Astronomical Data Analysis Software and Systems V, ed. G. Jacoby & J. Barnes (San Francisco: ASP), 17
Balucinska-Church, M., & McCammon, D. 1992, ApJ, 400, 699
Bardelli, S., Zucca, E., & Baldi, A. 2001, MNRAS, 320, 387
Bauer, F., & Sarazin, C. L. 2000, ApJ, 530, 222
Bazzano, A., et al. 1984, ApJ, 279, 515
Böhringer, H., et al. 1993, MNRAS, 264, L25
———. 2001a, A&A, 365, L181
———. 2001b, A&A, in press (astro-ph/0111112)
Burns, J. O. 1990, AJ, 99, 14
Calcáneo-Roldán, C., et al. 2000, MNRAS, 314, 324
Ciardullo, R., Bond, H. E., Sipior, M. S., Fullton, L. K., Zhang, C.-Y., & Schaefer, K. G. 1999, AJ, 118, 488
Colbert, E. J. M., & Mushotzky, R. F. 1999, ApJ, 519, 89
Dickey, J. M., & Lockman, F. J. 1990, ARA&A, 28, 215
Donahue, M., Mack, J., Voit, G. M., Sparks, W., Elston, R., & Maloney, P. R. 2000, ApJ, 545, 670
Edge, A. C. 2001, MNRAS, 328, 762
Fabian, A. C. 1994, ARA&A, 32, 277
Fabian, A. C., et al. 2000, MNRAS, 318, L65
Fabian, A. C., Mushotzky, R. F., Nulsen, P. E. J., & Peterson, J. R. 2001, MNRAS, 321, L33
Feretti, L., et al. 1999, A&A, 344, 472
Ferguson, H. C., Tanvir, N. R., & von Hippel, T. 1998, Nature, 391, 461
Flores, R. A., Quintana, H., & Way, M. J. 2000, ApJ, 532, 206
Forman, W., & Jones, C. 1982, ARA&A, 20, 547
Fusco-Femiano, R., et al. 1999, ApJ, 513, L21
———. 2000, ApJ, 534, L7
———. 2001, ApJ, 552, L97
Giovannini, G., Tordi, M., & Feretti, L. 1999, NewA, 4, 141
Gregg, M. D., & West, M. J. 1998, Nature, 396, 549

Guainazzi, M., & Molendi, S. 1999, A&A, 351, L19
Harris, D. E., et al. 2000, ApJ, 530, L81
Harris, W. E. 1991, ARA&A, 29, 543
Heckman, T. M., Baum, S. A., van Breugel, W. J. M., & McCarthy, P. J. 1989, ApJ, 338, 48
Hertz, P., & Wood, K. S. 1985, ApJ, 290, 171
Ikebe, Y., et al. 1997, ApJ, 481, 660
Irwin, J. A., & Sarazin, C. L. 1995, ApJ, 455, 497
Iwasawa, K., et al. 2000, MNRAS, 318, 879
Jaffe, W. 1990, A&A, 240, 254
Jaffe, W., & Bremer, M. N. 1997, MNRAS, 284, L1
Kaastra, J. S. 1992, An X-Ray Spectral Code for Optically Thin Plasmas (Internal SRON-Leiden Report, updated Version 2.0)
Kallman, T. R., Vrtilek, S. D., & Kahn, S. M. 1989, ApJ, 345, 498
Katz, J. I. 1976, ApJ, 207, 25
Liedahl, D. A., Osterheld, A. L., & Goldstein, W. H. 1995, ApJ, 438, L115
Loewenstein, M., Hayashida, K., Toneri, T., & Davis, D. S. 1998, ApJ, 497, 681
Lopez-Cruz, O., et al. 1997, ApJ, 475, L97
Markevitch, M., et al. 2000, ApJ, 541, 542
Markevitch, M., Forman, W. R., Sarazin, C. L., & Vikhlinin, A. 1998, ApJ, 503, 77
Markevitch, M., & Vikhlinin, A. 1997, ApJ, 491, 467
McNamara, B. R., Bregman, J. N., & O'Connell, R. W. 1990, ApJ, 360, 20
McNamara, B. R., et al. 2000, ApJ, 534, L135
Mewe, R., Gronenschild, E. H. B. M., & van den Oord, G. H. J. 1985, A&AS, 62, 197
Molendi, S., & De Grandi, S. 1999, A&A, 351, L41
Molendi, S., & Pizzolato, F. 2001, ApJ, 560, 194
Moore, B., Lake, G., Quinn, T., & Stadel, J. 1999, MNRAS, 304, 465
Mushotzky, R. F., & Szymkowiak, A. E. 1988, in Cooling Flows in Clusters and Galaxies, ed. A. C. Fabian (Dordrecht: Kluwer), 53
Nandra, K., et al. 1997, ApJ, 477, 602
Narayan, R., & Raymond, J. 1999, ApJ, 515, L69
Narayan, R., & Yi, I. 1995, ApJ, 452, 710
O'Dea, C. P., et al. 1994, ApJ, 422, 467
Oegerle, W. R., & Hill, J. M. 1994, AJ, 107, 857
Peres, C. B., et al. 1998, MNRAS, 298, 416
Peterson, J. R., et al. 2001, A&A, 365, L104
Rephaeli, Y. 2000, in AIP Conf. Proc. 558, High Energy Gamma-Ray Astronomy, ed. F. A. Aharonian & H. J. Völk (Melville: AIP), 427
Rephaeli, Y., Gruber, D. E., & Blanco, P. 1999, ApJ, 511, L21
Sambruna, R. M., et al. 2000, ApJ, 532, L91
Sarazin, C. L. 1996, in Galactic and Cluster Cooling Flows, ed. N. Soker (San Francisco: PASP), 115, 172
———. 2001, in Merging Processes in Clusters of Galaxies, ed. L. Feretti, M. Gioia, & G. Giovannini (Dordrecht: Kluwer), in press (astro-ph/0105418)
Sarazin, C. L., Burns, J. O., Roettiger, K., & McNamara, B. R. 1995, ApJ, 447, 559
Sarazin, C. L., & McNamara, B. R. 1997, ApJ, 480, 203
Snowden, S. L., et al. 1992, ApJ, 393, 819
Stark, A. A., et al. 1992, ApJS, 79, 77
Tamura, T., et al. 2001, A&A, 365, L87
Thompson, L. A., & Gregory, S. A. 1993, AJ, 106, 2197
Verbunt, F., Bunk, W., Hasinger, G., & Johnston, H. M. 1995, A&A, 300, 732
Voit, G. M., & Donahue, M. 1995, ApJ, 452, 164
West, M., Côté, P., Jones, C., Forman, W., & Marzke, R. 1995, ApJ, 453, L77
White, D. A., et al. 1991, MNRAS, 252, 72
White, D. A., Jones, C., & Forman, W. 1997, MNRAS, 292, 419
White, N. E., Stella, L., & Parmar, A. N. 1988, ApJ, 324, 363
Xu, H., et al. 1998, ApJ, 500, 738